J Electr Eng Technol Vol. 7, No. 6: 932-939, 2012
http://dx.doi.org/10.5370/JEET.2012.7.6.932

ISSN(Print) 1975-0102
ISSN(Online) 2093-7423

Electric Model of Li-Ion Polymer Battery for Motor Driving Circuit in Hybrid Electric Vehicle

June-Sang Lee*, Jae-Joong Lee*, Mi-Ro Kim, In-Jun Park*** Jung-Gu Kim***, Ki-Sik Lee§ and Wansoo Nah†**

Abstract – This paper presents an equivalent circuit model of a LIPB (Li-Ion Polymer battery) for Hybrid Electric Vehicles (HEVs). The proposed equivalent circuit can be used to predict the charging/discharging characteristics in time domain as well as the impedance characteristic analysis in frequency domain. Based on these features, a one-cell model is established as a function of Depth of Discharge (DoD), and a 48-cell model for a battery pack was also established. It was confirmed by experiment that the proposed model predict the discharging and impedance (AC) characteristics quite accurately at different constant current levels. To check the usefulness of the proposed circuit, the model was used to simulate a motor driving circuit with an Insulated Gate Bipolar Transistor (IGBT) inverter and Brushless DC (BLDC) motor, and it is confirmed that the model can calculate the battery voltage fluctuation in time domain at different DoDs.

Keywords: Li-Ion polymer battery, Equivalent circuit model, Depth of discharge, Open circuit voltage, Hybrid electric vehicle

1. Introduction

In the last few decades high-efficiency and eco-friendly electric vehicles have been under intense development due to the depletion of fossil fuels, and the air pollution problems that Internal Combustion Engines (ICEs) generate. Electric Vehicles (EV) use motors to drive a car by using the electrical energy charged in the battery, however, the commercialization of this big sized-battery has been difficult to be implemented due to its long charging time, short life span, heavy weight, and high price *etc*. In order to overcome these difficulties, various types of EVs are under development at domestic and overseas car makers [1]. EVs are built using a number of power electronic systems. In addition, high-voltage system has been employed in the EVs to improve the high electric power characteristics. Depending on the type of main power source, EVs can be classified into three classes: HEVs, PHEVs, and OLEVs. In Hybrid Electric Vehicles (HEVs), the motor is driven by a relatively small battery through the Regenerative Braking System (RBS) in the ICE. Because of the limitations of battery performance, the engine and motor are used together in combination. In Plug-in Hybrid Electric Vehicles (PHEVs), the battery is charged at the gas-station or home at night. PHEV is a fuel-efficient vehicle due to its reduced dependence on the ICE, as the battery is charged separately. In On-Line Electric Vehicles (OLEVs), the current collector, which is installed in the lower part of the vehicle, converts magnetic fields caused by a feeder constructed under the road into voltage [2]. The motor is driven by the power from the feeder as well as from the extra battery. Moreover, the battery weight and size can be reduced to one-fifth of the previous level, because the battery is used only for emergencies.

The HEVs, which have been the most actively developed among the EVs, have a more complex structure than the others. The proportion of power electronic circuits associated with power control is highly increased in HEVs. The major components of HEV are a high voltage battery, a booster converter to amplify voltage from the battery, a Battery Management System (BMS) to control a high voltage battery, an Insulated Gate Bipolar Transistor (IGBT) inverter to control a Brushless DC (BLDC) motor through Pulse Width Modulation (PWM), a generator to charge a battery through RBS, a DC-DC converter to convert high voltage into 12V, an DC-AC inverter to operate an air conditioner, and an Electrical Control Unit (ECU) to control all systems. The motor driving system in HEVs including mechanical components can be seen in Fig. 1. To analyze all the electric circuits mentioned above at design stage, it is crucial to have an accurate battery circuit model which can predict both charge/discharge characteristics, and the AC characteristics as well. So far, various battery models have been developed, and some models could explain the charging/discharging charac- teristics quite accurately in time domain [3], and the other models could explain the impedance characteristics quite all right

† Corresponding Author: School of information and communication engineering, Sungkyunkwan University, Korea. (wsnah@skku.edu)
* Dept. of electrical and electronic engineering, Sungkyunkwan University, Korea. (sincereljs@gmail.com)
** Dept. of computer aided engineering, Hyundai Mobis, Korea. (mrkim@mobis.co.kr)
*** Dept. of advanced material science and engineering, Sungkyun-kwan University, Korea. (kimjg@skku.ac.kr)
§ Dept. of electronic and electrical engineering, Dankook University, Korea. (kisiklee@dankook.ac.kr)
Received: December 1, 2011; Accepted: August 17, 2012

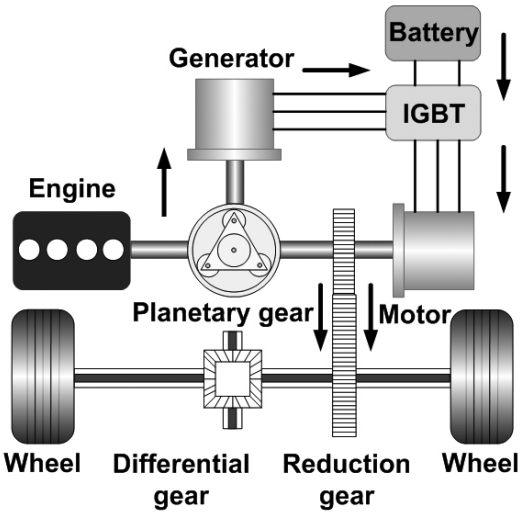

Fig. 1. Series-Parallel HEV System

in frequency domain [4]. But, as far as we know, no models have been proposed to explain both the time and frequency domain simultaneously. Since the motor-driving power electronic circuit consumes its power from the DC battery and also switches the devices at high frequency to control the circuit, it is very important to have an accurate battery model which can be used in both charging/discharging mode and for the AC impedance analysis as well. In this paper, a novel battery model is proposed which can predict both the charging/discharging and impedance (AC) characteristics. This paper has three main chapters. Some basic battery characteristics are introduced in chapter 2, and details on the battery modeling is described in chapter 3. Finally to check the validness of the proposed battery model, its application to motor driving system is described in chapter 4.

2. Battery Characteristics

The Lithium Ion Battery (LIB) is a kind of rechargeable battery. The battery has the feature that the lithium ion moves from the anode electrode to the cathode electrode in the electric discharge process. In the electric charging process, the lithium ion is returned to the origin, which is the anode electrode. The basic characteristic of the Lithium Ion Polymer Battery (LIPB) is the utilization of the gel type electrolyte instead of the fluid electrolyte used in the LIB. The other characteristic is that the energy density is high and the memory effect is low. In addition, the natural discharge is small enough in sleep mode. The LIPB can be divided into three parts, which are the anode, cathode and solid polymer electrolyte. A wide variety of materials are used in each part. The most widely used anode material is graphite. Lithium Cobalt Oxide (LiCoO2), Lithium Manganese Oxide (LiMn2O4), Lithium Iron Phosphate (LiFePO4), and *etc*. are mainly used as the cathode material and these are being actively developed.

In order to represent the electrochemical properties of the battery, the DoD-dependent parasitic resistance and capacitance should be known. The electron movement during discharging can be seen in Fig. 2. In this figure, energy levels are denoted as horizontal lines in each region of the battery. The Lowest Unoccupied Molecular Orbital (LUMO) is the energy level at which electrons are not filled. If the energy level in anode electrode is higher than the LUMO during charging, electron in cathode electrode moves towards electrolyte for reduction reaction. As a result, the difference in energy level for each material can be modeled as resistance. Electrolyte consists of three parts: bulk solution, diffusion layer, and SEI (Solid Electrolyte Interface). The diffusion layer is close enough to participate in a chemical reaction with the anode electrode. And, the bulk solution is far away to participate in a chemical reaction. The SEI is the surface film layer formed between the lithium-metal and electrolyte, and has the characteristics required for passing lithium ions, blocking the movement of electrons and inhibiting the self-discharge. An electric double-layer is between the positive charges in the anode electrode and the negative charges in electrolyte.

Using Fig. 2, an equivalent circuit can be formed.

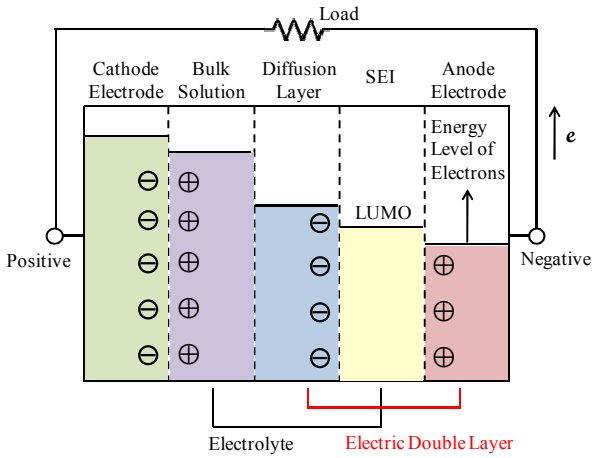

Fig. 2. Electron movement during discharging. Current flows in the opposite direction of electron movement.

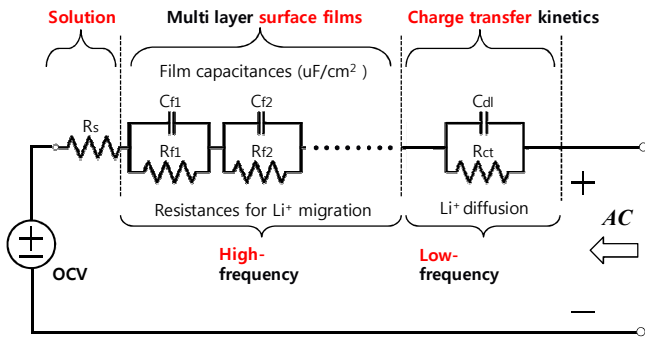

Fig. 3. Equivalent circuit model for ac impedance characteristics of LIPB

Basically the charged particles in the battery can be modeled by a capacitor, and a resistance can be used in the equivalent circuit when the battery has to work to make the current flow. In Fig. 3, charge transfer resistance (R_{ct}) is used to represent the work done to raise the energy level, and double layer capacitance (C_{dl}) is used for the charged particles on the electric double layer. The resistance and capacitance formed in SEI is called film resistance (R_f) and film capacitance (C_f) respectively. Solution resistance (R_s) is used to represent the resistance when charges move in the bulk solution. Fig. 3 shows finally obtained equivalent circuit, and Open Circuit Voltage (OCV) in the figure is the electric potential difference between the two terminals of a battery with no load.

3. Battery Modeling

3.1 Discharging voltage measurement in time domain

Fig. 4 shows the measurement setup with EIS (Electro-chemical Impedance Spectroscopy) to measure voltages and impedances during the charging/discharging period. The detailed measurement procedures are described in Table 1. When charging the battery up to maximum voltage (=4.25V), the Constant Current (CC) mode was used to keep the current constant. After reaching the cut-off current (=1/50C), the mode was changed into Constant Voltage (CV) Mode, making the current gradually reduced. When discharging the battery from the maximum voltage to the cut-off voltage (=2.5V), only the CC method is used. As the discharge progresses, impedance of the battery was measured at four State of Charge (SoC) levels: 75%, 50%, 25%, and 0%. Because of the limited capability of EIS we used, the OCV and impedance at 100% SoC were calculated using the equations, which were also verified by simulation. The SoC and Depth of Discharge (DoD) are the parameters to check battery charge status. DoD is inversely proportional to SoC: as one increases, the other one decreases. The relationships between SoC and DoD are defined by Eqs. (1) and (2). In addition, the relationships between measured voltage and SoC are defined by Eqs. (3) and (4). E is OCV, Q is the total cell charge, E_f is the maximum charge voltage of a cell, and E_e is the cut-off voltage of a cell.

$$SoC(t) = Q_t - \int_0^t i(\tau)d\tau \tag{1}$$

$$DoD(t) = \frac{Q_t - SoC(t)}{Q_t} = \frac{\int_0^t i(\tau)d\tau}{Q_t} \tag{2}$$

$$\begin{aligned} E &= E_f - DoD \times (E_f - E_e) \\ &= E_e + (E_f - E_e) SoC\% \end{aligned} \tag{3}$$

$$SoC\% = \frac{E - E_e}{E_f - E_e} \tag{4}$$

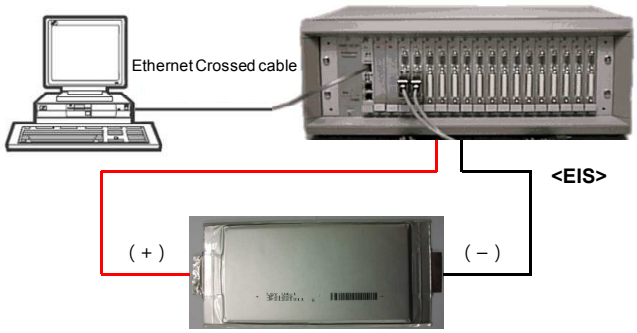

Fig. 4 Measurement setup with EIS

Table 1 Measurement procedure

No.	Subject	Test condition
①	1. Charge a cell to the max voltage (4.25 V) 2. Stand by 5 minutes	- Discharge Current : 1~5A
②	1. Measure Impedance at SoC 100% (4.2V) 2. Measure 3 times / Standby 5 minutes 3. Discharge	- Discharge Current : 1 A (Normal)
③	1. Measure Impedance at SoC 75% (3.8375V) 2. Measure 3 times / Standby 5 minutes 3. Discharge	- Discharge Current : 1 A (Normal)
④	1. Measure Impedance at SoC 50% (3.4750V) 2. Measure 3 times / Standby 5 minutes 3. Discharge	- Discharge Current : 1 A (Normal)
⑤	1. Measure Impedance at SoC 25% (3.1125V) 2. Measure 3 times / Standby 5 minutes 3. Discharge	- Discharge Current : 1 A (Normal)
⑥	1. Measure Impedance at SoC 0% (2.75V) 2. Measure 3 times / Standby 5 minutes	- Discharge Current : 1 A (Normal)

3.2 Open circuit voltage model in time domain

The OCV is the battery voltage when the external load is in its open state, which is dependent on the state of charge of the battery. Fig. 6 shows discharge characteristics *vs*. DoD at four current levels. Initially there is a sharp voltage drop between the two terminals when the battery is discharged in a CC mode. This region is called exponential zone. Subsequently, the voltage slowly decreases, and this region is called nominal zone, which is the normal operating region of the battery. Then, there is again a sharp voltage drop after the end of the nominal zone till the full discharge. The whole discharge curves can be expressed by Eq. (5), which has three terms. E_{full} is the full charge voltage of a cell (=4.2V), E_{Exp} is the voltage at the end of exponential zone (=3.7V), E_{nom} is the voltage at the end of nominal zone (=3.627V), and Q is the nominal capacity (=4Ah). A is the voltage drop at the exponential zone (=0.5V), B is the exponential zone time constant inverse (=2.5Ah^{-1}), Q_{Exp} is the discharge capacity at the end of exponential zone (=1.2Ah), and Q_{Nom} is the discharge capacity at the end of nominal zone (=3.2Ah). K is the

polarization voltage (=0.0187V), which is associated with the slope of voltage drop, and E_0 is the battery constant voltage (=3.74V). R is the solution resistance (=0.1025Ω) obtained from the impedance measurement, and i is the constant current (=0.2A). Consequently, E_0 can be expressed by Eq. (9) [5].

$$E = E_0 - K\frac{Q}{Q-\int_0^t i(\tau)d\tau} + A\cdot e^{\left(-B\cdot\int_0^t i(\tau)d\tau\right)} \quad (5)$$

$$E_{Full} = E_0 - K + A \qquad (t=0)$$

$$E_{Nom} = E_0 - K\frac{Q}{Q-Q_{Nom}} + A\cdot e^{(-B\cdot Q_{Nom})} \quad (6)$$

$$A = E_{Full} - E_{Exp}, \quad B = \frac{3}{Q_{Exp}} \quad (7)$$

$$K = \frac{\left(E_{Full} - E_{Nom} + A\left(e^{(-B\cdot Q_{Nom})} - 1\right)\right)}{Q_{Nom}}\cdot\left(Q - Q_{Nom}\right) \quad (8)$$

$$E_0 = E_{full} + K + R\cdot i - A \quad (9)$$

The battery specifications are described in Table 2, and Fig. 6 shows the measured discharging voltages as well as the calculated and simulated voltages. In this figure, calculation was done using (5), and the simulation was performed using (16), and ANSYS Simplorer and Matlab (MathWorks) were used for the simulation and calculation.

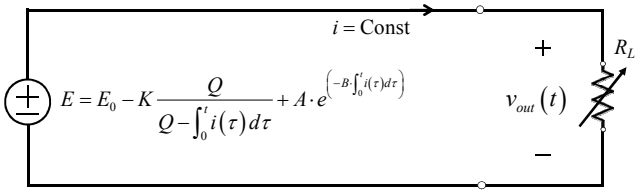

Fig. 5. Open Circuit Voltage Model in time domain

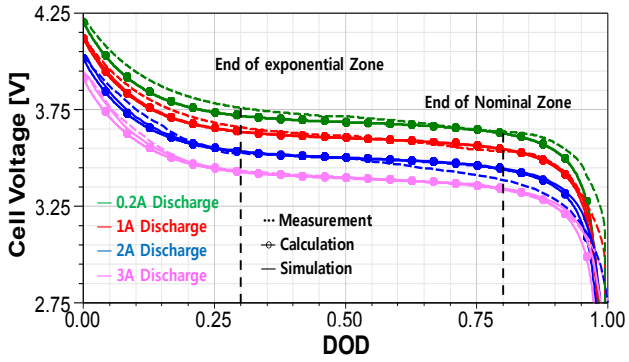

Fig. 6. Discharging characteristics *vs*. DoD for one-cell model at four constant currents. (5) is used for the calculation, and (16) is used for the simulated voltages.

Table 2 Specifications of LIPB of one cell

Item		Rating	Note
Nominal Capacity		4000mAh	Discharge : 0.2C Cut off voltage : 2.75 V
Cut off Voltage		2.75 V	
Nominal Voltage		3.7 V	
Charge Current	Standard	0.2 mA	
	Rapid	0.5 mA	
Charge Voltage		4.2 V	Cut off current : 0.05 mA
Maximum Charge Voltage		4.25 V	

3.3 Electrochemical parameter (AC Impedance) measurement in frequency domain

To extract the electrochemical parameters AC impedance method has been usually used, and these impedances are measured by employing small AC voltage across battery in a wide range of frequencies. Fig. 7 shows measured impedances from 5mHz to 1KHz at different DoDs, and these traces are called Nyquist plot. With these data, the circuit parameters in Fig. 3 can be identified as a function of DoDs. In this paper, seven parameters (R_s, R_{ct}, R_{f1}, R_{f2}, C_{dl}, C_{f1}, C_{f2}) could be identified at several DoD levels: 100%, 75%, 50%, 25%, and 0%. To get smooth functions with respect to DoD, interpolation techniques have been used.

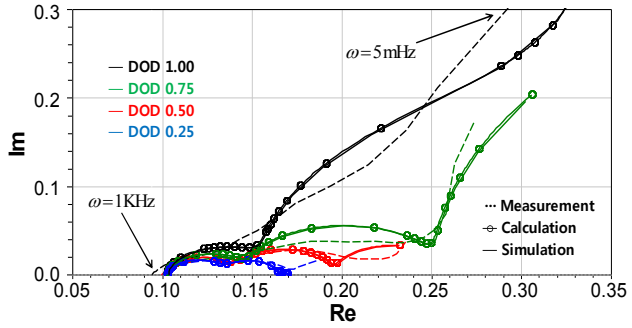

Fig. 7. Nyquist plots for one-cell at four DoD levels. Fig. 3 and Fig. 10 were used for the calculation and simulation, respectively.

For the resistances, exponential interpolation was used, and the results are summarized in (10-12). For the capacitances, Newton's divided-difference interpolating polynomial was used [6], and the final interpolated functions are described in (13-15). Consequently, the resistance and capacitance are defined as functions of DoD, and the measured, calculated, and simulated results are depicted in Fig. 8 and 9.

$$R_{ct} = \left(0.45720\cdot e^{9.9570\cdot DoD}\right)\cdot 10^{-3} \quad (10)$$

$$R_{f1} = \left(0.02694 \cdot e^{0.6509 \cdot DoD}\right) \quad (11)$$

$$R_{f2} = \left(0.01572 \cdot e^{2.5230 \cdot DoD}\right) \quad (12)$$

$$C_{dl} = \left(1220 \cdot DoD^2\right) - \left(2721 \cdot DoD\right) + 1508 \quad (13)$$

$$C_{f1} = \left(0.1636 \cdot e^{0.1666 \cdot DoD}\right) + \left(0.008504 \cdot e^{2.506 \cdot DoD}\right) \quad (14)$$

$$C_{f2} = \left(11.15 \cdot DoD^4\right) - \left(25.32 \cdot DoD^3\right) + \left(14.35 \cdot DoD^2\right) - \left(0.3706 \cdot DoD\right) + 3.75 \quad (15)$$

Table 3 Extracted Parameters at several DoDs

DoD	0	0.25	0.5	0.75	1
V	4.25 V	3.8375 V	3.4750 V	3.1125 V	2.75 V
Rs [Ω]	0.1022	0.1025	0.1026	0.1048	0.0988
C_{f1} [F]	0.1725	0.1739	0.1797	0.2004	0.2427
R_{f1} [Ω]	0.0254	0.0331	0.0398	0.0428	0.0513
C_{f2} [F]	3.7504	4.2921	4.6843	4.3901	3.5602
R_{f2} [Ω]	0.0207	0.0347	0.0641	0.0902	0.2002
C_{dl} [F]	1500	866.2	420.6	164.1	7.5
R_{ct} [Ω]	0.0121	0.0280	0.0582	0.8015	9.6510

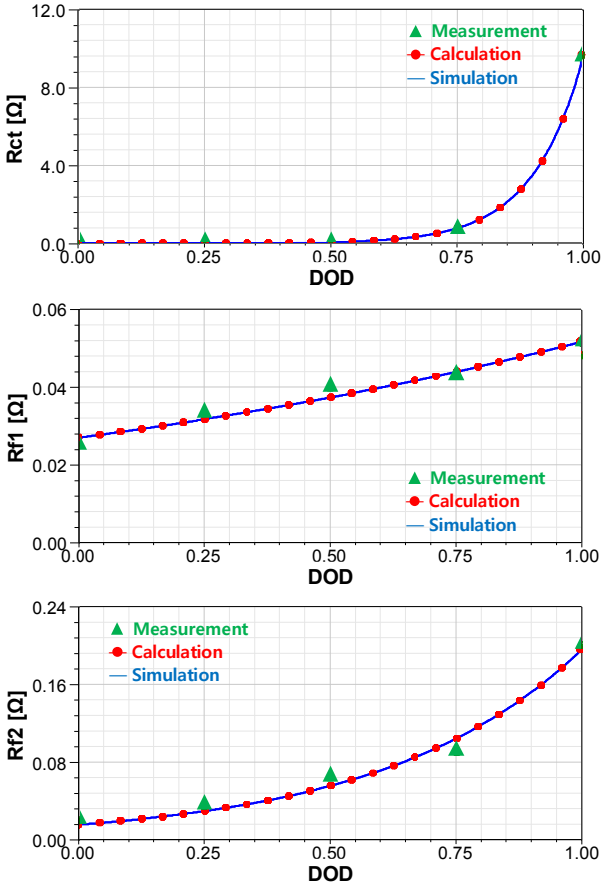

Fig. 8. Interpolated charge transfer resistance (R_{ct}) and film resistance (R_{f1} and R_{f2})

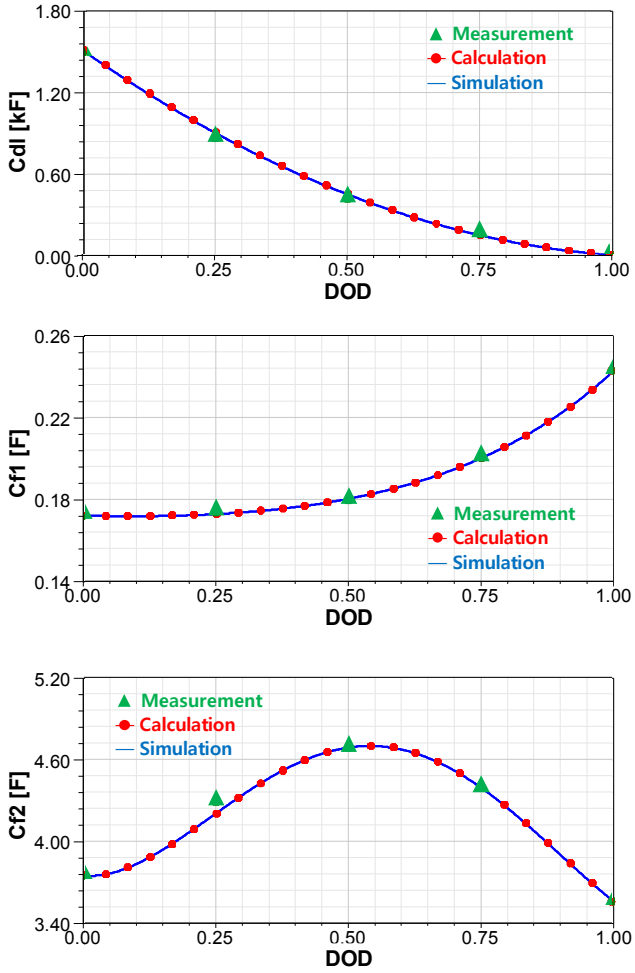

Fig. 9. Interpolated Double layer capacitance (C_{dl}) and film capacitance (C_{f1} and C_{f2})

3.4 Combined model

The battery model to be used for feeding power electronics circuit should be able to predict the discharging characteristics of Fig. 6 as well as the battery internal impedance characteristics in Fig. 7. A combination of Fig. 6 and 7 is described in Fig. 10, and this is the battery circuit model this paper proposes. The output voltage at the load can be represented as

$$v_{out}(t) = E_0 - K\frac{Q}{Q - \int_0^t i(\tau)d\tau} + A \cdot e^{\left(-B \cdot \int_0^t i(\tau)d\tau\right)} - v_{internal}(t) \quad (16)$$

where $v_{internal}(t)$ is the voltage drop across the seven *R and C* elements, and notice that these elements were introduced to characterize the ac impedance of Fig. 7. So (16) is the modified version of (5) with $v_{internal}(t)$ thrown in. Even with this additional voltage drop, (7) and (8) can still be used for

the evaluation of constants K, A, and B. This is because the load resistance R_L is adjusted to get a constant current during discharging process, so the introduction of the resistances of R_s, R_{f1}, R_{f2}, and R_{ct} with constant current condition does not change anything in the circuit. Moreover, since the typical discharging period is in the order of an hour, the capacitances in Fig 10 do not have any effect on the time-varying output voltage $v_{out}(t)$: that is, from Table 3, the maximum time constant of parallel R-C circuit is in the order of seconds, which is very fast compared to the discharging time scale. The simulated curves in Fig. 6 are obtained from (16), and one can find they coincide very nice to the measured ones at different current values. Also Fig. 10 was used for the simulated impedances in Fig. 7, and they also coincide quite well with the measured impedance characteristics.

In real EVs the batteries are cascaded to get high voltages to drive the power electronic circuits. Fig. 11 and 12 show impedance and discharging characteristics of cascaded 48-cell batteries packed together. R_S of the 48-cell model is 4.9215Ω at 1KHz, and the full charge voltage of 202V. Each result is 48 times as large as that of one-cell and in the next section these curves are used to simulate the responses of the motor driving circuit in EVs.

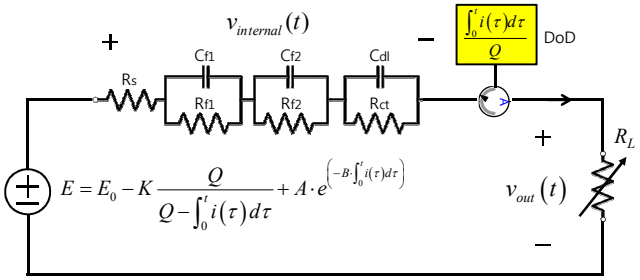

Fig. 10. Combined equivalent circuit model for LIPB

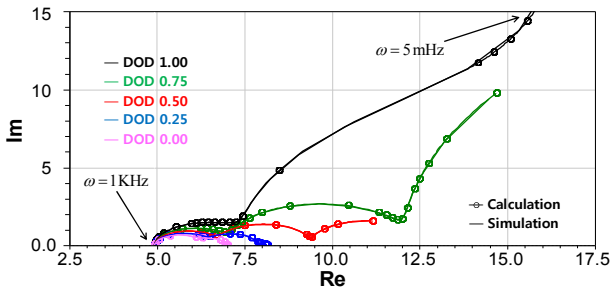

Fig. 11. Nyquist plot results for 48-cell model

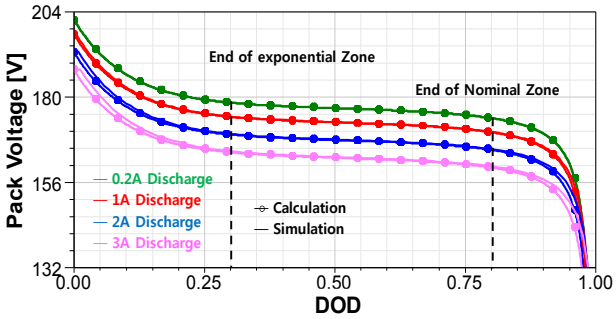

Fig. 12. OCV results for 48-cell model

4. Estimation of Voltage Fluctuation in Motor Driving Circuit

When high power switching devices such as IGBT and Power Metal-Oxide Semiconductor Field Effect Transistor (MOSFET) are implemented for a BLDC motor in an electric vehicle, noises induced from the switching devices are conducted to the source, making the source voltage fluctuated. This noise makes Electromagnetic Interference

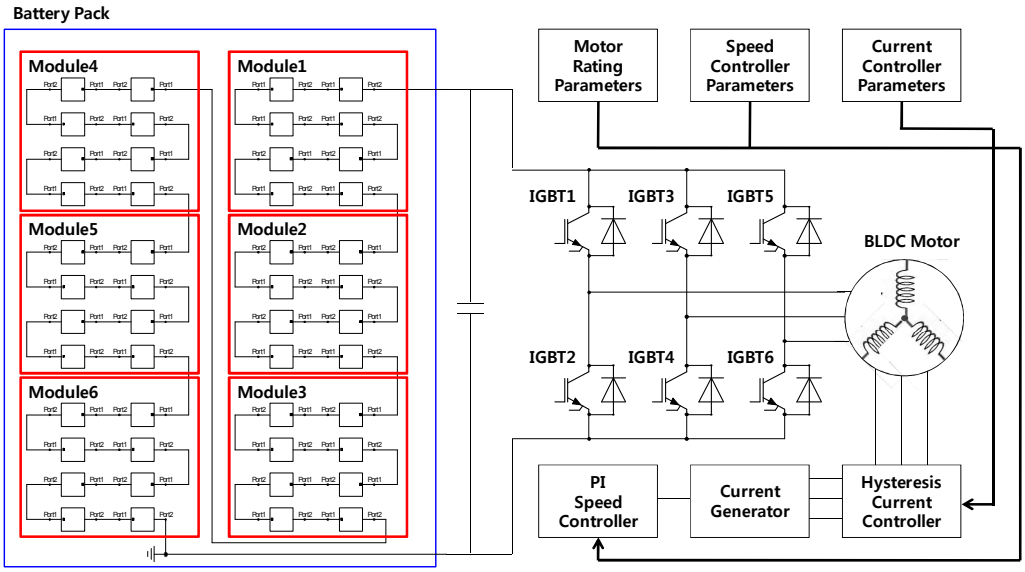

Fig. 13 Battery pack simulation model including BLDC motor and IGBT inverter

(EMI), and needs to be minimized at the circuit design stage, of course [7, 8]. In order to predict battery voltage fluctuations, one needs an equivalent circuit for the battery which can reproduce the discharging characteristics at different current levels and the impedance characteristics as well. The simulation and modeling procedure which includes BLDC motor as well as IGBT switching devices is shown in Fig. 13. The battery pack has 6 modules consisting of 8 battery cells for each module. Cells in the battery pack were connected in series and PI speed controller was used for BLDC motor control. Fig. 14 shows the simulated battery voltage fluctuation in a motor driving circuit using the proposed battery model at DoD=0. The switching frequency of IGBT in the simulation is 20KHz, and the rated power of the BLDC motor is 30KW (=40HP) with its rated speed of 3500rpm. If an ideal voltage source of zero internal impedance is used, the battery voltage does not fluctuate, keeping constant voltage as the blue line in Fig. 14. The peak-to-peak voltage of the battery pack is about 40V. Also shown in Fig. 15 is the simulated battery voltage fluctuation at DoD=0.3. Since the pack voltage is around 180V at DoD=0.3 from Fig. 12, one can see that the battery voltage is fluctuating around 180V.

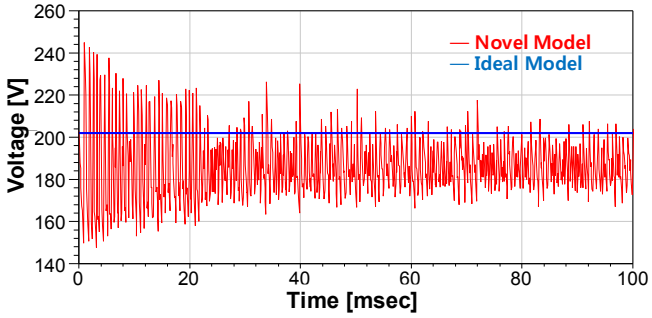

Fig. 14. Simulated battery voltage fluctuation in motor driving circuit using the proposed battery model at DoD=0. The constant line represents the voltage from ideal voltage model

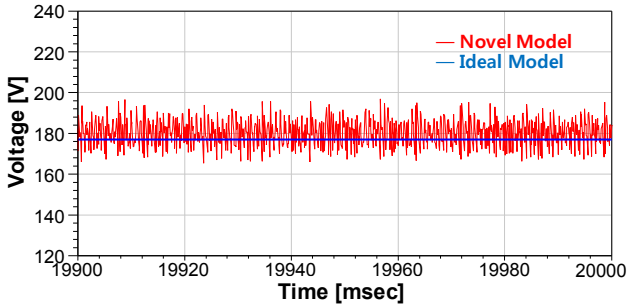

Fig. 15. Simulated battery voltage fluctuation in motor driving circuit using the proposed battery model at DoD=0.3. The constant line represents the voltage from ideal voltage model

5. Conclusion

In this paper an equivalent circuit model of an LIPB was presented. For the prediction of battery voltages at charging/discharging period in time domain, open circuit voltage model was used, and the constants in the model could be determined from the experimental data. The open circuit voltage model was able to predict the discharging voltages quite correctly even at different current levels. To characterize electrochemical properties of the LIPB, ac impedance model should also be established. From the experimentally obtained impedance data in a Nyquist diagram, DoD-dependent resistances and capacitances could be successfully identified and interpolated, and the ac impedance characteristics could be reproduced using the DoD-dependent circuit model. In this paper the OCV and AC impedance models were integrated into one, and it was verified that the proposed model reproduce the discharging voltages in time domain and ac impedance in Nyquist diagram quite accurately. Finally to check the usefulness of the proposed battery model, the model was applied to a BLDC motor driving circuit to find that it could show the voltage fluctuation quite all right even at different DoD levels. We think that the proposed novel battery model could be of great help to estimate the conducted noises as well as the voltage fluctuation in a battery-driven power circuit at different DoD levels.

Acknowledgements

This work was supported by the Human Education Program for Green Car Electrotechnology of the Korea Institute of Energy Technology Evaluation and Planning (KETEP) grant funded by the Korea government Ministry of Knowledge Economy (No. 20104010100630-12-1-000)

References

[1] C.C. Chan, “The State of the Art of Electric, Hybrid, and Fuel Cell Vehicles”, *Proceedings of the IEEE*, pp. 704-718, April, 2007.

[2] N. P. Suh, D. H. Cho, C. T. Rim, “Design of On-line Electric Vehicle (OLEV)”, *Plenary lecture at the 2010 CIRP Design Conference, France*, April 2010.

[3] Il-Song Kim, “The novel state of charge estimation method for lithium battery using sliding mode observer”, *Journal of Power Sources*, Vol. 163, Issue 1, pp. 584-590, December 2006.

[4] B. Y. Liaw, G. Nagasubramanian, R. G. Jungst, D. H. Doughty, “A frequency-domain approach to dynamical modeling of electrochemical power sources”, *Electro-chimica Acta*, Vol. 47, Issues 13-14, pp. 2347-2356, May 2002.

[5] O. Tremblay, L. -A. Dessaint, A. -I. Dekkiche, "A Generic Battery Model for the Dynamic Simulation of Hybrid Electric Vehicles", *Vehicle Power and Propulsion Conference (VPPC), IEEE*, pp. 284-289, September 2007.
[6] S. C. Chapra, R. P. Canale, *Numerical Methods for Engineers*: Mcgraw-Hill Education 5th edition, 2008, Chapter 17.
[7] S. Chen, T. W. Nehl, J.-S. Lai, X. Huang, E. Pepa, R. De Doncker, I. Voss, "Towards EMI prediction of a PM motor drive for automotive applications", *Applied Power Electronics Conference and Exposition (APEC), Eighteenth Annual IEEE*, pp. 14-22, February 2003.
[8] Jin Hur, Byeong-Woo Kim, "Rotor Shape Design of an Interior PM Type BLDC Motor for Improving Mechanical Vibration and EMI Characteristics", Journal of Electrical Engineering & Technology, Vol. 5, No. 3, pp. 462~467, 2010.

June-Sang Lee He received his B.S. degree in electrical engineering from Myongji University, Korea, in 2010. Since 2010, he has worked for his M.S. degree in department of electrical and electronic engineering at Sungkyun kwan University. His research interests include Signal Integrity (SI), Power Integrity (PI) in system level and Electro- magnetic Interference (EMI) reduction in Hybrid Electric Vehicle (HEV).

Jae-Joong Lee He received his B.S. degree in semiconductor science from Dongguk University, Korea, in 2010. Since 2011, he has worked for his M.S. degree in department of electrical and electronic engineering at Sungkyun kwan Uni-versity. His research interests include His research interests include Electromagnetic Compatibility (EMC) and battery modeling for HEV/EV.

Mi-Ro Kim He received his B.S. and M.S. degree in mechanical engineering from Chung-Ang University, Korea, in 1994 and 1996, respectively. He was a research engineer at Deawoo Research Institute in Yongin, Korea from 1996 to 2003. Since 2004, he has been a principal research engineer at Hyundai Mobis in yongin, Korea. His primary interests are Signal Integrity (SI), Power Integrity (PI), and Electro-magnetic Interference (EMI) in Electric Vehicle.

In-Jun Park He received his B.S. degree in school of advanced materials science and engineering from Sung kyunkwan Uni-versity, Korea, in 2008. Since 2008, he has worked for his M.S. degree and Ph.D. degree in school of advanced materials science and engineering at Sungkyunkwan Uni-versity. His primary interests are electrochemical corrosion and batteries evaluation.

Jung-Gu Kim He received his B.S. degree in metallurgical engineering from Sung-kyunkwan University, Korea, in 1984 and his M.S., and Ph.D. degree in materials science and engineering from Tennessee State University, USA, in 1988, and 1992 respectively. He was a postdoctoral researcher at University of Tennessee, Knoxville in USA from 1992 to 1994, and was a senior researcher at KIST (Korea Institute of Science and Technology) in Seoul, Korea from 1994 to 1995. Since 1995, He has been a professor in school of advanced material science and engineering at Sungkyunkwan University in Suwon, Korea. His primary interests are electrochemical corrosion and reliability evaluation.

Ki-Sik Lee He received his B.S., M.S., and Ph.D. degree in electrical engineering from Seoul National University, Korea, in 1973, 1977, and 1985, respectively. He has been a professor in department of electronic and electrical engineering at Dankook University in Yongin, Korea. His primary interests are analysis and design of electrical machine, Surge Protection Devices (SPD), energy saving techniques in Hybrid Electric Vehicles.

Wansoo Nah He received his B.S., M.S., and Ph.D. degree in electrical engineering from Seoul National University, Korea, in 1984, 1986, and 1991 respectively. He was a guest researcher at SSCL (Super- conducting Super Collider Laboratory) in USA from 1991 to 1993, and was a senior researcher at KERI (Korea Electrical Research Institute) in Changwon, Korea from 1993 to 1995. Since 1995, He has been a professor in school of information and communication engineering at Sungkyunkwan University in Suwon, Korea. His primary interests are Signal Integrity (SI), Power Integrity (PI) on the board and chip level, and development of Electromagnetic Interference (EMI) reduction technique through SI and PI enhancement.